This article has been accepted for publication in a future issue of this journal, but has not been fully edited. Content may change prior to final publication. Citation information: DOI 10.1109/TCSII.2016.2604425, IEEE Transactions on Circuits and Systems II: Express Briefs

On the Dual-Frequency Impedance/Admittance Characteristic of Multi-Section Commensurate Transmission-Line

Mohammad A. Maktoomi, *Graduate Student Member, IEEE*, M. Akbarpour , *Member, IEEE*, Mohammad S. Hashmi, *Member, IEEE*, Fadhel M. Ghannouchi, *Fellow, IEEE*

***Abstract*—In this paper, firstly, an interesting dual-frequency feature of multi-section commensurate transmission-line is reported. The property concerns with the impedance (or admittance) looking into such multi-section transmission-line terminated with a real impedance. Rigorous mathematical analysis is provided to prove the existence of the property. Secondly, as an application, novel multi-section dual-frequency impedance transformer for the real impedance is presented. The proposed transformer can be used to provide matching over much wider transformation-ratio that is otherwise impossible to realize using current state-of-the-art of dual-frequency transformers. The EM simulated and measured results exhibit good performance.**

***Index Terms*—Baluns, dual-frequency, impedance matching.**

I. Introduction

THE rapid growth in the software-defined/cognitive radio (SDR/CDR) technologies [1] has led to an enormous interest in the dual-/multi-frequency impedance matching networks [4]-[13]. Moreover, their design and development have become even more important because of the rise of interests in simultaneous harvesting energy from multiple sources [14].

Monzon two-section transformer [2] has established itself as a *de facto* real-to-real dual-frequency impedance transformer. Such transformer is useful in dual-frequency components such as in power amplifiers [1], in baluns [3] and in complex-to-real impedance transformers [12]. However, the limited transformation ratio/band-ratio ($=f_2/f_1$) remains a major challenge in their design and development.

In this brief, we show a unique dual-frequency impedance/admittance property of multi-section commensurate transmission-line. Moreover, their potential application in dual-frequency impedance matching problem is also discussed and demonstrated.

Manuscript received May 01, 2016, Revised July 14, 2016, Accepted July 28, 2016. "This work was supported by IIIT Delhi overseas research fellowship, NSERC Discovery grant, Canada Research Chair Grant, and Alberta Innovate Technology Futures Chair grant".

M. S. Hashmi and M. A. Maktoomi are with the CDRL, IIIT Delhi, New Delhi, 110020, India, and also with the iRadio Lab, University of Calgary, Calgary, AB, T2N 1N4, Canada(e-mail:{ayatullahm, mshashmi}@iiitd.ac.in).

M. Akbarpour and F. M. Ghannouchi are with the iRadio Lab (email: makbarpo@ucalgary.ca, fghannou@ucalgary.ca).

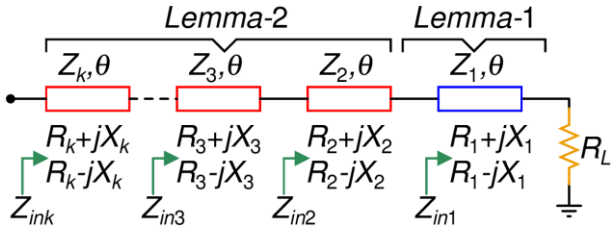

Fig. 1. Multi-section TL terminated into a real impedance.

II. The Property and its Proof

A multi-section commensurate transmission-line (TL) structure is shown in Fig. 1. Z_{ini} is the characteristic impedance of i^{th} TL section, whereas θ is the electrical length of each section, $i \in [1, k]$ beginning from the right, and k is the total number of TL sections. The dual-frequency impedance property of this multi-section structure is stated as follows:

"*The impedance, Z_{ink}, looking into the multi-section transmission-line is complex conjugate of each other at the two frequencies f_1 and f_2, that is, $Z_{ink}|_{f_1} = (Z_{ink}|_{f_2})^*$, and vice-versa, if the value of θ is selected as follows:*

$$\theta = m\pi/(1+r), m \in \text{Integer}, r = f_2/f_1 ." \quad (1)$$

Moreover, since admittance is just the inverse of impedance, the above dual-frequency property also holds true for the input admittance. The proof of the above property is based on the following two lemmas.

A. *Lemma*-1

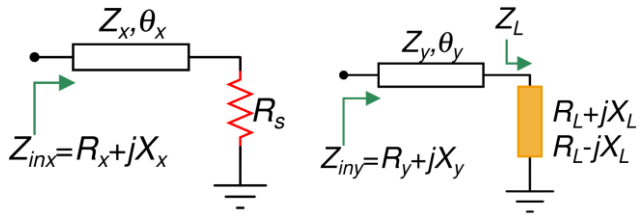

Fig. 2. A TL section terminated into (a) a real impedance (b) complex conjugate impedance.

Consider Fig. 2(a), where a TL section having characteristic impedance Z_x and electrical length θ_x is terminated into a real impedance R_s. Z_{inx} is the input impedance looking into this structure. Then, the lemma-1 is stated as follows:

"*If θ_x is chosen as θ, that is, the same as given in (1), then*

$Z_{inx}\big|_{f_1} = (Z_{inx}\big|_{f_2})^*$, *and vice-versa."*

Proof: Applying the formula of input impedance for a transmission-line in Fig. 2(a), Z_{inx} can be expressed as follows:

$$Z_{inx} = Z_x \frac{R_s + jZ_x \tan\theta_x}{Z_x + jR_s \tan\theta_x} = R_x + jX_x \tag{2}$$

where,

$$R_x = \frac{R_s Z_x^2 \left(1+\tan^2\theta_x\right)}{Z_x^2 + R_s^2 \tan^2\theta_x} \tag{3}$$

$$X_x = \frac{Z_x \left(Z_x^2 - R_s^2\right)\tan\theta_x}{Z_x^2 + R_s^2 \tan^2\theta_x} \tag{4}$$

A quick look at the above expression reveals that if θ_x is replaced by $m\pi$-θ_x, then R_x remains the same, whereas just the sign of X_x gets changed. Therefore, if θ_x is the electrical length assigned to the TL at the first frequency, f_1, and it is chosen in such a manner that the corresponding electrical length at the second frequency, f_2, is $m\pi$-θ_x, then we can write the following expressions considering that electrical length is proportional to frequency:

$$\theta_x = k_1 f_1 \tag{5}$$

$$m\pi - \theta_x = k_1 f_2 \tag{6}$$

where, k_1 is some constant with unit of rad/Hz.
Solving (5) and (6) for θ_x gives the following expression:

$$\theta_x = m\pi/(1+r), m \in \text{Integer}, r = f_2/f_1 \tag{7}$$

B. *Lemma*-2

Consider Fig. 2(b), where a TL section having characteristic impedance Z_y and electrical length θ_y is terminated into an impedance Z_L, which has complex conjugate relation at two frequencies, that is, $Z_L\big|_{f_1} = (Z_L\big|_{f_2})^*$. Z_{iny} is input impedance looking into this structure. Then, the lemma-2 is stated as follows:

"If θ_y is chosen as θ, that is, the same as given in (1), then $Z_{iny}\big|_{f_1} = (Z_{iny}\big|_{f_2})^*$, and vice-versa."

Proof: Applying the formula of input impedance for a transmission-line in Fig. 2(b), and after subsequent rationalization the following expressions are obtained:

$$R_y\big|_{f_1} = \frac{R_L Z_y^2 (1+\tan^2\theta_y)}{(Z_y - X_L\tan\theta_y)^2 + (R_L\tan\theta_y)^2} \tag{8}$$

$$X_y\big|_{f_1} = Z_y \frac{(X_L + Z_y\tan\theta_y)(Z_y - X_L\tan\theta_y) - R_L^2\tan\theta_y}{(Z_y - X_L\tan\theta_y)^2 + (R_L\tan\theta_y)^2} \tag{9}$$

Now, considering the fact that an electrical length θ defined at f_1 becomes $r\theta$ at f_2; $R_y\big|_{f_2}$ and $X_y\big|_{f_2}$ are obtained from (8) and (9) by replacing θ_y with $r\theta_y$, and X_L with $-X_L$. Then, it is apparent from (8) and (9) that for $Z_{iny}\big|_{f_1} = (Z_{iny}\big|_{f_2})^*$ to hold true, one must ensure $\tan r\theta_y = -\tan\theta_y$, and this requires that θ_y is given as follows:

$$\theta_y = m\pi/(1+r),\ m \in \text{Integer}, r = f_2/f_1 \tag{10}$$

Now, applying the lemma-1 and lemma-2 in Fig. 1 proves the dual-frequency impedance property of the multi-section line.

III. Application of the Property

The classic two-section Monzon transformer [2], which can be considered as a special case of the proposed multi-section transformer has no independent (free) variable, as is apparent from (19) - (20) of [2]. This fact limits the range of load (and thus, the transformation-ratio $K = Z_0/R_L$) that can be matched using the same. Here, R_L is the load impedance whereas $Z_0 = 50\Omega$ is the source impedance. To illustrate this issue, plots of the line impedances of the Monzon transformer against the load impedance are shown in Fig. 3 for $r = 1.5$, 2, and 3.5. Two scenarios are considered: the load impedance is larger than the source impedance ($K < 1$, Fig. 3(a)), and the load impedance is smaller than the source impedance ($K > 1$, Fig. 3(b)). It is evident from Fig. 3 that as R_L moves below 15Ω or beyond 240Ω, the required values of either or both of the line impedances are less than 20Ω or greater that 150Ω. Typically, the realizable characteristic impedance of microstrip lines that can be fabricated lies between 20Ω to 150Ω. Thus, it is clear that Monzon two-section transformer is very limited in many scenarios. And, therefore, in the next subsections potential of the dual-frequency impedance property to mitigate this limitation is investigated.

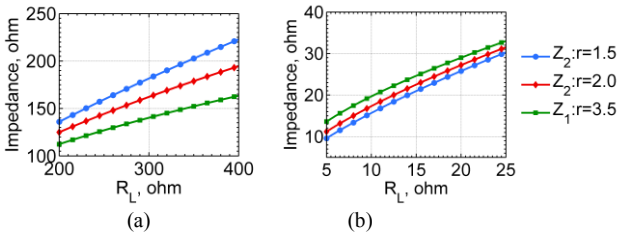

Fig. 3. The variation of line impedances with the load impedance in Monzon transformer for r =1.5, 2 and 3.5, when (a) $R_L > Z_0$ (b) $R_L < Z_0$.

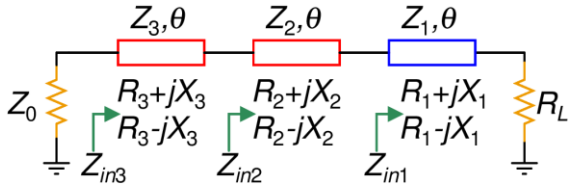

Fig. 4. Proposed tri-section dual-frequency impedance transformer.

A. *Proposed Tri-Section Dual-Frequency Transformer*

The proposed tri-section dual-frequency impedance transformer is shown in Fig. 4. As depicted, Z_{ini} , $i = \{1,2,3\}$ is the input impedance looking into the i^{th} transmission line beginning from the right. Moreover, since θ is to be chosen according to (1), therefore, Z_{ini}, $i = \{1,2,3\}$ has the complex conjugate relation at the two frequencies. The expression of R_1 and X_1 can be obtained using (3) and (4) by replacing R_s with R_L, Z_x with Z_1, and θ_x with θ.

This article has been accepted for publication in a future issue of this journal, but has not been fully edited. Content may change prior to final publication. Citation information: DOI 10.1109/TCSII.2016.2604425, IEEE Transactions on Circuits and Systems II: Express Briefs

Now, using the formula of input impedance we have the following expressions for the shown tri-section network:

$$Z_{in2} = Z_2 \frac{R_1 + jX_1 + jZ_2 \tan\theta}{Z_2 + j(R_1 + jX_1)\tan\theta} \tag{11}$$

$$Z_{in3} = Z_3 \frac{Z_{in2} + jZ_3 \tan\theta}{Z_3 + jZ_{in2} \tan\theta} \tag{12}$$

Eliminating Z_{in2} from (11) and (12) and invoking $Z_{in3}=Z_0$, the following equations are obtained with $a = \tan\theta$.

$$Z_0 a^2 Z_2^2 + [Z_0 X_1 a + Z_3(R_1 - Z_0)]Z_2 + [Z_3 Z_0 X_1 a - Z_3^2 R_1 a^2] = 0 \tag{13}$$

$$Z_3 a Z_2^2 + [Z_3 X_1 - R_1 Z_0 a + Z_3^2 a]Z_2 - [Z_3 Z_0 R_1 a + Z_3^2 X_1 a^2] = 0 \tag{14}$$

Eliminating Z_2 from (13) and (14) results into a 4th-order equation in Z_3:

$$AZ_3^4 + BZ_3^3 + CZ_3^2 + DZ_3 + E = 0 \tag{15}$$

where:

$$A = \frac{R_1^2 a^4}{Z_0} - p_1(R_1 - Z_0)\frac{R_1 a}{Z_0} - R_1 p_1^2 a^2 \tag{16}$$

$$B = p_1 X_1 (R_1 - Z_0)(1 + a^2) + p_1^2 Z_0 X_1 a - p_1 X_1 R_1 a^2 - 2X_1 R_1 a^3 (1 + a^2) \tag{17}$$

$$C = Z_0 X_1^2 a^2 (1 + a^2)^2 - 2Z_0 R_1^2 a^4 + 2p_1 Z_0 R_1^2 a^3 + R_1^2 (R_1 - Z_0)a^2 + p_1 Z_0 X_1^2 a(1 + a^2) + p_1 R_1 Z_0 (R_1 - Z_0)a \tag{18}$$

$$D = 2Z_0^2 R_1 X_1 a^3 (1 + a^2) + R_1^2 X_1 a^3 - Z_0 R_1 X_1 (R_1 - Z_0)a(1 + a^2) - p_1 Z_0^2 R_1 X_1 a^2 \tag{19}$$

$$E = Z_0^3 R_1^2 a^4 - Z_0^2 R_1 X_1^2 a^2 (1 + a^2) - Z_0^2 R_1^2 (R_1 - Z_0)a^2 - Z_0^2 R_1^3 a^4 \tag{20}$$

$$p_1 = a + \frac{1}{a}\left(1 - \frac{R_1}{Z_0}\right) \tag{21}$$

This 4th-order equation of (15) can be solved for Z_3 and subsequently, Z_2 is obtained form (13) and (14) as follows:

$$Z_2 = \frac{Z_0 R_1 a Z_3 + X_1(1 + a^2)Z_3^2 - \frac{R_1 a}{Z_0} Z_3^3}{p_1 Z_3^2 - Z_0 R_1 a} \ . \tag{22}$$

Regarding the proposed tri-section dual-frequency transformer, following comments are in order:

1) Solution of (15) and (22) depends on R_1 and X_1 which in turn depends on Z_1. Therefore, Z_1 is a free variable which provides flexibility to the proposed tri-section transformer. This free variable is not present in the Monzon two-section transformer. In fact, the proposed tri-section transformer is a more generic form of Monzon transformer. Specifically, when the electrical length of the TL having characteristic impedance Z_1 tends to zero (i.e. when this TL is short-circuited), the proposed transformer reduces to the Monzon transformer as $X_1=0$ and $R_1=R_L$ in this scenario.
2) Z_1 is a free yet a bounded variable; its value is selected appropriately in the range [20Ω, 150Ω] until realizable values of Z_2 and Z_3 are obtained.

IV. Generic Multi-Section Transformer Design

After discussing working of the proposed tri-section dual-frequency impedance transformer, it is now easier to extend the same to multi-section transformer case. The following guidelines can be used to access the required design equations. For the proposed tri-section dual-frequency impedance transformer, Z_3 and Z_2 are the variables to be determined and Z_1 is assumed to be a free variable. On a similar line, for quad-section transformer, Z_4 and Z_3 are to be determined and Z_2 and Z_1 can be assumed to be free variables. In general, for a k-section transformer of Fig. 1, Z_k and Z_{k-1} are to be determined and Z_{k-2}, Z_{k-3}, ..., and Z_1 are assumed to be free variables. Now, in order to determine Z_k and Z_{k-1}, one simply needs to replace Z_3 and Z_2 in (15) and (22) with Z_k and Z_{k-1}, and R_1 and X_1 with R_{k-2} and X_{k-2}, respectively. The required values of R_{k-2} and X_{k-2} in a multi-section transformer are now functions of Z_{k-2}, Z_{k-3}, ..., and Z_1, and they can readily be obtained using (3) - (4), and recursive use of (8) - (9).

V. Simulation and Discussion

Figs. 5 and 6 depict the line impedance variations in the proposed tri-section impedance transformer for different values of r =1.5, 2 and 3.5. The scenario when $R_L > Z_0$ has been considered in Fig. 5, and $R_L < Z_0$ in Fig. 6. These plots have been obtained using the equations derived in the previous section and letting Z_1 to assume any value between 20Ω to 150Ω. Comparing these plots with the Monzon two-section transformer response shown earlier in Fig. 3, it is apparent that the required line impedances falls within the realizable impedance. Specifically, it must be noted of the required characteristics impedances are neither below 20Ω nor above 150Ω. It is to be appreciated that the acceptable solution is possible for R_L as low as 5Ω and as high as 400Ω. Please also note that since Z_1 is a free variable, Figs. 5 and 6 just show one of the possible profiles for each scenario. The abrupt change in line impedances shown in Fig. 6(f), near R_L=12Ω, has no special significance except that a valid solution is not available until Z_1 assumes a value near the lower impedance bound allowed.

Next, since there are more than one free variable for quad-/higher-section transformer, it is more meaningful to show their potential using few examples. To that end, Table I shows few examples of the proposed quad-section transformer with their corresponding simulation results in Fig. 7. The proper dual-frequency behavior is apparent. Thanks to the availability of two free design variables (Z_1 and Z_2) now, the parameters of quad-section transformer can be more easily realized in microstrip.

At this juncture, we wish to draw the reader's attention to other interesting three-section designs reported earlier in [10]-[11]. The proposed tri-section transformer is distinctively different from that reported in [10] in the following ways:

This article has been accepted for publication in a future issue of this journal, but has not been fully edited. Content may change prior to final publication. Citation information: DOI 10.1109/TCSII.2016.2604425, IEEE Transactions on Circuits and Systems II: Express Briefs

1) The earlier reported transformer cannot match a real impedance to another real impedance. Specifically, it must be noted that substituting R_a=R_b=R_L in equation (13) of [10] does not yield a realistic solution.
2) The concept of the proposed tri-section transformer emanates from a more generalized and easily comprehensible dual-frequency admittance property of multi-section transmission line discussed in Section II. Therefore, it can be extended to, say, a four-section transformer, while [10] cannot.

The tri-section transformer reported in [11] is, in fact, a tri-frequency impedance transformer. However, [11] is limited to tri-section design only and cannot be extended to multi-section scenario. Furthermore, since [5] and [9] utilize basic equations derived in [10], therefore, they cannot be used for real load impedance. Specifically, this limitation becomes apparent from [eqn. (9), [5]] by setting $G_a = G_b$, and from [eqn. (4), [9]] by setting $R_{L1} = R_{L2}$. While [8] requires an optimization algorithm to arrive at a solution, [7] is a quad-frequency transformer based on two-sections of C-type coupled lines. Difference between these various designs is summarized in Table II.

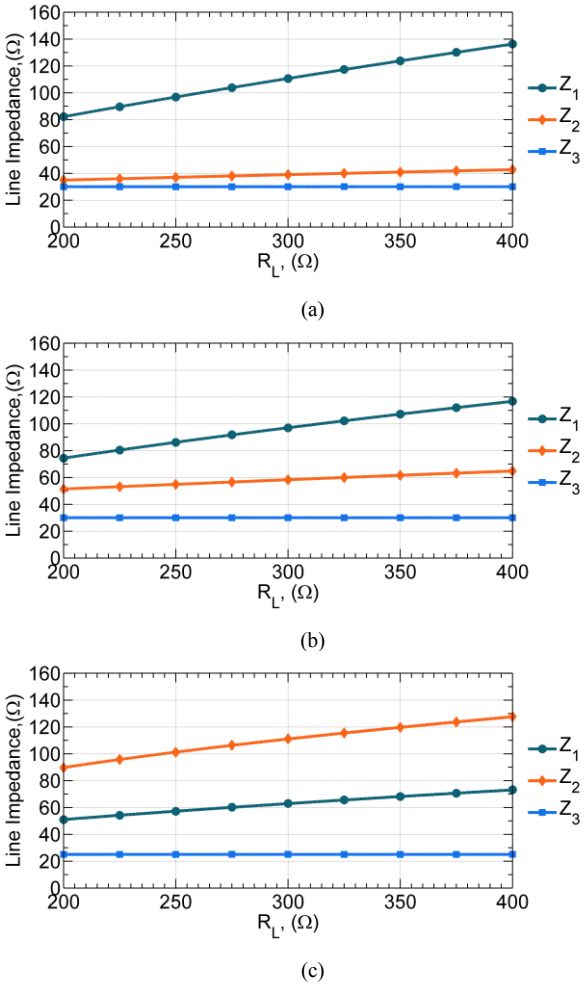

Fig. 5. Line impedance variation for the proposed tri-section dual-frequency impedance transformer, when R_L>Z_0 and (a) r =1.5, (b) r =2, and (c) r =3.5.

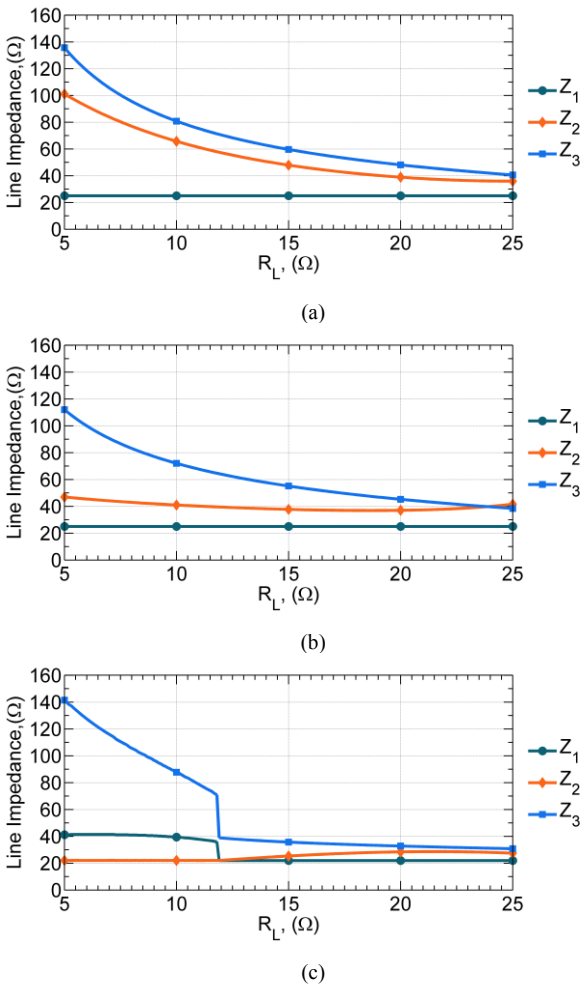

Fig. 6. Line impedance variation for the proposed tri-section dual-frequency impedance transformer, when R_L<Z_0 and (a) r =1.5, (b) r =2, and (c) r =3.5.

TABLE I
LINE IMPEDANCE OF QUAD-SECTION TRANSFORMER, R_L=400Ω

r	Z_1 (Ω)	Z_2 (Ω)	Z_3 (Ω)	Z_4 (Ω)
1.5	100	40	42.34	77.31
2.0	70	60	37.38	99.12
3.5	71.1	105.2	30.05	30.01

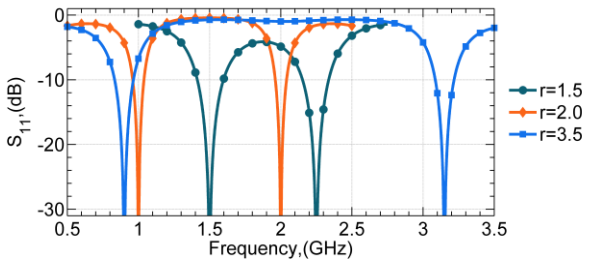

Fig. 7. Return loss of the proposed quad-section transformer.

VI. PROTOTYPES AND MEASUREMENT RESULTS

Three designs of the proposed tri-section impedance transformers are implemented on Roger's RO4003C substrate having dielectric constant ϵ_r =3.55 and substrate height of 0.8mm on 35μm copper cladding as shown in Fig. 8(a). These designs have been numbered as 'A', 'B' and 'C'. l_i and w_i, i={1,

2, 3} represents the length and width of the i^{th} section for each design. The complete details of each design are mentioned in Table III. A 10Ω resistor has been used for design 2, since still a lower value is not available. Design equations derived in the previous sections have been used to find the appropriate transmission line parameters. Subsequently, the Keysight ADS LineCalc® is used to find the physical dimension of each TL. To compensate for steps between the TL sections, and to take deviations due to the use of high frequency resistor model; optimization is performed. The final dimensions (in mils) of various TL sections of each design are listed in Table III. Since, each design is a single-port network; N5230A PNA-L 13.5 GHz network analyzer is used to measure S_{11} as depicted in Fig. 8(b). The measured return loss of each design is shown in Fig. 8(c). A concurrent working at the two frequencies is apparent, and the return loss is higher than 15 dB for each design at either frequency.

TABLE II
COMPARISON WITH PREVIOUS TECHNIQUES

Ref. No.	Freq bands	Real Load	Multi-Sections
[2]	two	Yes	No
[5]	two	No	No
[7]	four	Yes	No
[8]	two	Yes	No
[9]	two	No	No
[10]	two	No	No
This work	two	Yes	Yes

TABLE III
DESIGN PARAMETERS OF THE PROTOTYPE (DIMENSIONS: MILS)

No.	r, f_1(GHz)	R_L(Ω)	l_3/w_3	l_2/w_2	l_1/w_1
A	r =1.5, f_1=1.5	402	916.4/211	888.8/154.4	908.4/17.2
B	r =2.0, f_1=1.0	10	1246.6/18.2	1170.4/61.6	1063.7/125
C	r =3.5, f_1=0.9	402	1734.9/153.5	909.9/17.6	43.57
Part No. for R_L:		CRCW0603402RFKEA (402Ω) CRCW060310R0FKEA (10Ω)			

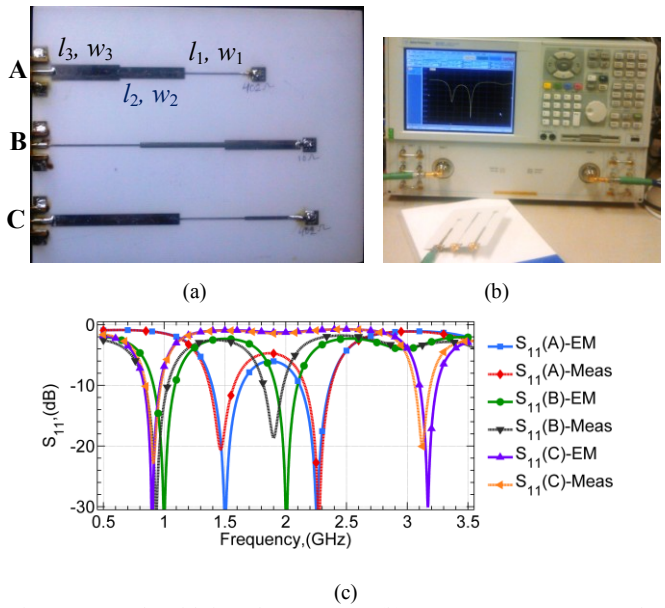

Fig. 8. (a) The fabricated prototype, (b) measurement setup, and (c) comparison of return losses obtained from EM-simulation and measurement.

Considering 15dB reference, the minimum achievable bandwidth of 61MHz occurs for the design C at f_2. This bandwidth is good figure for dual-frequency applications [13]. It should be also be noted that insertion loss is direct function of the return loss assuming that no radiation/ conductive/ dielectric losses exist in structure. As discussed in [14], these losses are often negligible at low RF frequencies and for transmission line based structures built properly in low loss dielectric substrate.

VII. CONCLUSION

In this paper, theory and application of dual-frequency impedance property of multi-section commensurate transmission-line was presented. Rigorous mathematical analysis was carried out to derive the design equations. The presented theory can potentially be applied to overcome the limited transformation-/frequency-ratios of the current-state-of-the-art designs.

REFERENCES

[1] K. Rawat, M. S. Hashmi, and F. M. Ghannouchi, "Dual-band RF circuits and components for multi-standard software defined radios," *IEEE Circuits Syst. Mag.*, vol. 12, no. 1, pp. 12–32, Feb. 2012.

[2] C. Monzon, "A small dual-frequency transformer in two sections," *IEEE Trans. Microw. Theory Tech.*, vol. 51, no. 4, pp. 1157–1161, Apr. 2003.

[3] H. Zhang, Y. Peng, and H.Xin, "A tapped stepped-impedance balun with dual-band operations," *IEEE Antennas Wireless Propag. Lett.*, vol.7, pp. 119–122, 2008.

[4] Y. Wu, L. Jiao and Y. Liu, "Comments on "novel dual-band matching network for effective design of concurrent dual-band power amplifiers"," *IEEE Trans. Circuits Syst. I, Reg. Papers*, vol. 62, no. 9, pp. 2361–2361, Aug. 2015.

[5] O. Manoochehri, A. Asoodeh, and K. Forooraghi, "Pi -model dual-band impedance transformer for unequal complex impedance loads," *IEEE Microw. Wireless Compon. Lett.*, vol.25, no.4, pp.238–240, Apr. 2015.

[6] S. C. Dutta Roy, "Characteristics of single- and multiple-frequency impedance matching networks," *IEEE Trans. Circuits Syst. II, Exp. Briefs*, vol. 62, no. 3, pp. 222–225, Mar. 2015.

[7] Y. -F. Bai, X. -H. Wang, C. -J. Gao, Q. -L. Huang, and X. -W. Shi, "Design of compact quad frequency impedance transformer using two-section coupled line," *IEEE Trans. Microw. Theory Tech*., vol. 60, no. 8, pp. 2417–2423, Aug. 2012.

[8] M. -L. Chuang, "Dual-band impedance transformer using two-section shunt stubs," *IEEE Trans. Microw. Theory Tech*., vol.58, no.5, pp. 1257–1263, May 2010.

[9] Y. Wu, Y. Liu, S. Li, C. Yu, and X. Liu, "A generalized dual-frequency transformer for two arbitrary complex frequency-dependent impedances," *IEEE Microw. Wireless Compon. Lett*., vol.19, no.12, pp.792–794, Dec. 2009.

[10] X. Liu, Y. Liu, S. Li, F. Wu, and Y. Wu, "A three-section dual-band transformer for frequency-dependent complex load impedance," *IEEE Microw. Wireless Compon. Lett.*, vol. 19, no. 10, pp. 611–613, Oct. 2009.

[11] M. Chongcheawchamnan, S. Patisang, S. Srisathit, R. Phromloungsri, and S. Bunnjaweht, "Analysis and design of a three-section transmission-line transformer," *IEEE Trans. Microw. Theory Techn*., vol. 53, no. 7, pp. 2458−2462, Jul. 2005.

[12] M. A. Maktoomi, M. S. Hashmi, and V. Panwar, "A dual-frequency matching network for FDCLs using dual-band λ/4-lines," *Prog. Electromagn. Res.-L (PIER L)*, vol. 52, pp. 23-30, 2015.

[13] K. Rawat and F.M. Ghannouchi, "Dual-band matching technique based on dual-characteristic impedance transformers for dual-band power amplifiers design," *IET Microwaves, Antennas & Propagation*, vol.5, no.14, pp.1720–1729, Nov. 18, 2011.

[14] M. A. Maktoomi, M. S. Hashmi, and F. M. Ghannouchi, "Improving load range of dual-band impedance matching networks using novel load-healing concept," *IEEE Trans. Circuits Syst. II, Exp. Briefs*, 2016, available online in IEEExplore, DOI: 10.1109/TCSII.2016.2551547.